Biomedical Signal Processing and Control 108 (2025) 107966

Contents lists available at ScienceDirect

Biomedical Signal Processing and Control

journal homepage: www.elsevier.com/locate/bspc

An innovative web-based approach to generate respiratory biofeedback using virtual reality headset and embedded inertial sensors during an imposed breathing protocol: a proof-of-concept study

Andrea Carpi [a,b], Sarah Solbiati [a], Valentino Megale [c], Enrico Gianluca Caiani [a,d,*]

[a] *Electronics, Information and Bioengineering Dpt., Politecnico di Milano 20133 Milano, Italy*
[b] *Pukenga Srl, Parma, Italy*
[c] *Softcare Studios Srls, Rome, Italy*
[d] *IRCCS Istituto Auxologico Italiano, Ospedale San Luca, Milan, Italy*

ARTICLE INFO

Keywords:
Virtual reality
Respiration
Head-ballistocardiography
Web-oriented approach
Biofeedback
Digital health

ABSTRACT

Assessing impact of VR immersive scenarios on users, objective biometrics are measured by external sensors, interfering with subject's behavior and preventing outside laboratory applications. Micro-electromechanical systems embedded in VR headsets allow measuring biomarkers such as respiratory rate by exploiting head-related micro-movements by head-ballistocardiographic (HBCG) technique. We aimed at conducting a proof-of-concept study by developing a device-independent web-based imposed breathing VR experience during which the HBCG signal was acquired. Duration of respiratory cycle ($tRESP_{HBCG}$) during such VR experience was estimated in quasi-real time, thus allowing potential use in ecological momentary assessment of emotion elicitation.

Twenty-six healthy volunteers were recruited for the VR experience: they were asked, while sitting, to breath at different frequencies (4 s, 6 s, 8 s, 10 s per breath, corresponding to 15, 10, 7.5, and 6 respiratory cycles/ min) following an audio-visual guide. The HBCG signals were recorded and given as input for parameters identification to a grey-box algorithm to optimize the $tRESP_{HBCG}$ estimation, by using as reference the respiratory rate derived from simultaneously acquired 1-lead ECG. The optimized algorithm run on an online server to provide quasi real-time results. It was tested on 8 additional volunteers, reaching an absolute estimation error below 4 %. In addition, robustness analysis results showed good ability of the implemented algorithm in providing accurate results also in presence of noise. The proposed web-based approach resulted feasible and accurate, opening up new opportunities to create VR immersive scenarios and applications to measure biofeedback, with potential use in ecological momentary assessment of emotion elicitation and in respiratory training.

1. Introduction

Virtual Reality (VR) is an innovative technology that has revolutionized the landscape of computing and gaming in recent years. It creates an immersive, computer-generated virtual environment (VE) that simulates a physical environment, allowing the users to interact with it in a highly realistic way [1,2]. Lately, VR has garnered widespread attention in numerous fields. Particularly, in the healthcare sector, the use of VR is experiencing an exponential growth, as evidenced by the increasing number of relevant publications in PubMed over the past five years (search string "VR in Healthcare": 85 in 2018 vs. 261 in 2023). Applications in healthcare include physical rehabilitation [3], psychiatric treatment for specific phobias and post-traumatic stress disorder [4], pain management [5], anxiety and general stress during painful medical procedures [6,7,8,9], disaster medicine [10], patient education [11], and the training of healthcare workers [12], among others.

The impact of the quality of the VR experience (QoE) on the user, namely "the degree of delight or annoyance of the user of an application or service" [13], appears crucial in this context. Indeed, the QoE is intricately connected to users' emotions, sense of presence, induced stress levels, and engagement [14,15,16], making its assessment especially important considering the goals of the experience, and holding the potential to be utilized as feedback for refining and personalizing the

* Corresponding author.
E-mail address: enrico.caiani@polimi.it (E.G. Caiani).

https://doi.org/10.1016/j.bspc.2025.107966
Received 3 February 2024; Received in revised form 3 March 2025; Accepted 14 April 2025
Available online 26 April 2025

overall VR experience.

Various methods can be utilized to measure user QoE within the VE, including both explicit and subjective (based on post-test questionnaires [17,18]), as well as implicit and more objective approaches (based on the acquisition of physiological signals [19]). A potential framework for this evaluation, recently been proposed as a possible foundation for emotion-driven product design [20,21], is the VR-based Emotion-Recognition-Emotion-Elicitation Loop (VEE-loop), which involves emotion elicitation through a VE, the measurement of biofeedback, relevant emotion recognition, and dynamic modification of the VE. A current limitation of this approach is the necessity to equip the subject with multiple sensors (such as electrodes for electrocardiography, electromyography, electrodermal activity, chest strap for respiratory activity, etc.) to derive relevant features from the induced physiological response. This setup, however, not only is extremely time-consuming and potentially disruptive to the subject's normal behavior, but also potentially prevents the application of the VEE-loop in everyday-life scenarios outside the research laboratory [22].

In the context of measuring main physiological parameters such as heart rate (HR) and respiratory rate (RESPR), novel approaches have been proposed in the last decade, exploiting the body micro-movements synchronized with heart function and respiratory activity. This is made possible by the use of Micro Electronic Mechanical Systems (MEMS), embedding accelerometers and gyroscopes. Such sensors can also be placed on the subject's head, to measure the so-called Head Ballisto-cardiography (HBCG).

In 2011, He et al. introduced a method to measure HBCG using a portable device equipped with a 3-axial accelerometer, allowing for the derivation of HR [23,24]. Utilizing consumer-grade devices like Google Glasses, Hernandez et al. demonstrated in 2015 [25] the feasibility of measuring mean HR and RESPR in various positions (sitting, standing, and supine) under both relaxed and aroused (post-cycling) conditions. This was achieved through signal analysis in the frequency domain applied to the HBCG [26]. More recently, a machine learning approach was proposed to reconstruct respiratory signals from MEMS embedded in a Seaway smart glasses prototype while performing several common activities (sleeping, watching videos, talking, walking, and typing), all reproduced in a laboratory setting.

As regards the utilization of the VR headset for the measurement of HBCG signals, our recent research [27] has successfully demonstrated, for the first time, the feasibility of utilizing a commercial device (Oculus Go) with embedded MEMS as a passive sensor to measure head micro-movements in a controlled respiration protocol guided by an external audio, from which mean heart rate (HR) and respiratory rate (RESPR) could be estimated through simple frequency domain signal processing. This approach opens the possibility to potentially eliminate the need of using additional wearable devices to measure such parameters, as a way to obtain user biofeedback directly from the VR headset towards the implementation of the VEE-Loop. Subsequent to this study, we have expanded our research [28] to assess the feasibility of measuring the mean HR from inter-beat intervals obtained by beat-to-beat analysis of the acquired HBCG signal, also comparing results with those obtained using a monoaxial high-performance gyroscope [29].

Notably, the approaches described so far still lack the capability for near-real-time processing of the acquired HBCG signals, as they required custom software and/or hardware to run, due to the computationally-intensive offline processing, thus preventing a real-time biofeedback to the subject. This limitation confines their application to laboratory research, and their reliance on a low-level technological stack often involves advanced control over signal sampling, which was possible to achieve only via a custom hardware [23,24], or via a custom low-level executable [27,28]. In the context of our VR study [27], for example, MEMS signal recording relied on a device-specific application installed on the VR headset, with manual data transfer at the end of acquisition, thus excluding broader adoption for general purposes.

Given these considerations, we hypothesized that leveraging emerging open-source web libraries could facilitate the development of a fully web-based VR experience, without the need for neither a custom hardware not a low-level executable software. Such an experience, designed to be device-independent, would enable the users to immerse themselves in a 3D virtual scenario, respond to specific stimuli, and receive quasi-real-time feedback on their performance through the processing of the HBCG signal, potentially during an every-day web navigation. Accordingly, in this proof-of-concept study, our goal was to create a web-based VR experience where subjects follow an imposed breathing protocol for a specified duration during which the HBCG signal is acquired using the MEMS embedded in a commercial VR headset, and the mean duration of the respiratory cycle ($tRESP_{HBCG}$) is estimated in quasi-real time thanks to cloud processing. This approach aims to enable ecological momentary assessment of emotion elicitation through a VE, representing an initial step towards the realization of the VEE-Loop.

2. Materials and methods

The study was divided into two phases. In Phase 1, the primary objective was to implement and test a web-based approach to record data from the headset's MEMS, while properly tuning the proposed signal processing method to estimate the $tRESP_{HBCG}$. To determine its accuracy, this estimation was compared with both the imposed breathing period and $tRESP_{ECG}$ derived from the concurrently acquired ECG signals, as an additional reference.

In Phase 2, the focus was to create a fully functional web-based VR experience capable of measuring the user performance, by returning a score between 0 and 100, indicating how accurately the user followed an imposed breathing protocol. Also in this phase, the measured $tRESP_{HBCG}$ was compared with the imposed breathing period and with $tRESP_{ECG}$, and served as external validation of the proposed algorithm. In addition, an analysis of the robustness of the implemented strategy in the estimation of the respiratory frequency was performed by adding noise of different amplitude to the acquired signal.

2.1. Study Population

A total of 34 healthy volunteers were recruited: 26 initial participants (14 males and 12 females, age 26.15 (mean) $\pm$ 2.44 (standard deviation) years old, height 171 $\pm$ 8 cm, weight 64 $\pm$ 10 kg, Body Mass Index (BMI) 21.6 $\pm$ 2.3) to collect initial data from the prototype application for algorithm tuning (Phase 1). For Phase 2, 8 additional volunteers (4 males and 4 females, age 25.62 $\pm$ 3.81 years old, height 170 $\pm$ 10 cm, weight 65 $\pm$ 11 kg, BMI 22.7 $\pm$ 2.7) to test the VR experience and its performance (Phase 2).

All subjects provided voluntary written, informed consent to the experimental protocol approved by the Ethical Committee of the Politecnico di Milano (date of approval: 28 July 2022, number 29/22) in accordance with the Declaration of Helsinki of 1975, as revised in 2000.

2.2. Experimental design

2.2.1. The experimental design is the same in both Phase 1 and Phase 2

The experiments were performed in resting condition while seated, in order to minimize motion artifacts which could have occurred in a more dynamic environment, and each participant was asked to wear a commercial head-worn VR device (Oculus Quest, Oculus, Meta, USA) (Fig. 1). The headset embeds MEMS, by which the linear accelerations (m/s^2) of the head along the lateral (X, left-to-right), longitudinal (Y, foot-to-head) and transverse (Z, front-to-back) directions are sensed, as well as the angular rotations (rad/s) around such axes (pitch, yaw and roll, respectively for X, Y and Z).

Subjects were also instrumented with the EcgMove 4 (Movisense, Gmbh) sensor, which was positioned on the chest by means of dry electrodes.The device embeds a single-lead ECG sensor (sampling

Fig. 1. Left: Volunteer wearing the VR headset, embedding the inertial sensors from which the head ballistocardiography (H-BCG) signals are derived, while starting the protocol in sitting position, Right: representation of the ECGMove4 sensor, attached by two electrodes on the thorax, utilized to acquire the ECG, from which the reference respiratory signal was then obtain, as well as the inertial signals, utilized for synchronization purposes with the H-BCG obtained by the VR headset.

frequency 1024 Hz) and a triaxial inertial measurement unit (sampling frequency 64 Hz): it was used to derive the reference respiratory signal from the ECG, as well as for synchronization purposes.

2.3. Phase 1: Experimental protocol

In Phase 1, the experimental protocol delivered as VE experience consisted of four levels of a paced breathing exercise, each one including 12 respiratory acts with a specific breathing period, respectively of 4, 6, 8, and 10 s per breath (corresponding to the breathing frequencies of 15, 10, 7.5 and 6 respiratory cycles per minute). Both at the start and at the end of each level, the volunteer was instructed to perform a small jump, intended to produce a visible artifact in both the accelerometric signals recorded by the EcgMove 4, and by the accelerometers embedded in the headset [27,28,29]. These artefacts were later utilized in the pre-processing phase to properly synchronize the acquired signals. Fig. 2 shows a schematization of such experimental protocol.

2.4. Web app for the respiratory rate protocol

The software infrastructure that allowed the acquisition, processing, and storage of the subjects' data consisted of a client-side and a server-side. The client-side was structured as a JavaScript application running on the Oculus Quest headset via Oculus Browser, and in charge of the acquisition of the accelerometer's and gyroscope's data. The processing and storage were entrusted to an external server, thus benefitting from much higher computational and storage resources with respect to a commercial VR system. To avoid connection issues, instead of a continuous stream of data between the client and the server, the internet connections were limited to the beginning of the acquisition, when the HTML, JavaScript and visual/audio contents were downloaded from the internet, and at the end of each level, when the client-side uploads the recorded data to the server side.

The experimental protocol was embedded in an "ad hoc" web app reachable via Oculus Browser. The web page was developed in HTML and JavaScript: HTML was used to display static content, while JavaScript enabled calculations, changes in the graphical aspect, and sending and receiving operations to and from the external server. On top of

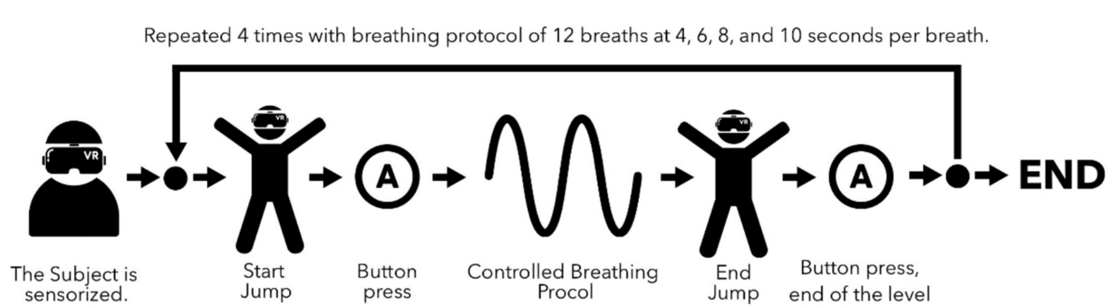

Fig. 2. Schematic representation of the conducted protocol of imposed breathing: 1) Initial jump for synchronization purposes; 2) Button pressed on the controller; 3) Start of the imposed breathing protocol; 4) End of the imposed breathing protocol; 5) Final jump for synchronization purposes.

JavaScript, Three.js and WebXR libraries were used for the creation of 3D and VR content.

The web app VE consisted of a virtual human-size room with light grey walls where the only stimuli provided to the subject were a visual and an audio guide. For the visual guide, a geometrical shape (i.e., a sphere) was used. To avoid motion sickness, the shape was left still, without any rotation, with changes in its size synchronous with a sinusoidal frequency corresponding to the imposed breathing frequency, from the smallest size (end of expiration) to the largest one (end of inspiration). To facilitate the user to follow the imposed breathing, the maximum and minimum extension of the sphere were always visible as overlays, so that the subject could understand how to modulate his breathing within such boundaries.

For the audio guide, a sound consisting of an ascending tone followed by a descending one, of the same duration, was used and played in.mp3 format on the headset. The visual and the audio guides were aligned to start together as the breathing protocol begins, and to stop exactly after twelve breaths for each imposed breathing level.

During each level, the web app acquired from the embedded MEMS sensors the position and orientation of the subject's head with respect to the initial position and orientation of the device, sampled at the web app start, with a sampling rate of 71.43 Hz (every 14 ms). Such data, along with the timestamps associated to the acquired samples, were stored locally on the headset and, at the end of each level, sent to the server in a.CSV format, secured via cryptography using the HTTPS protocol.

2.5. Phase 1: Data processing for parameters optimization

To be able to provide an estimate in quasi-real-time of the length of each breathing period ($tRESP_{HBCG}$) from the signals acquired by the MEMS sensors embedded in the VR headset, a fast, lightweight algorithm to be run on cloud, based on predefined parameters values, needed to be developed. To this purpose, with the aim to define the best combination and setting for such parameters (comparing the results with the respiratory information obtained by the ECG) to be then embedded in the lightweight algorithm, an approach based on a grey-box parameter identification was implemented using the data acquired in Phase 1, to optimize the setting of four specific parameters: p1, defining the best combination of input signals (i.e., the 3-axis components of both the accelerometer and rotational signals); p2, defining the order of a Moving Average filter applied to smooth the noisy input signal; p3, defining the number of consecutive applications of such filter; p4, defining the allowed minimum temporal distance between consecutive peaks in the filtered signal. This process will be explained in detail in the following section 2.5.3. Once the optimal parameters were identified, the algorithm was converted to Hypertext Preprocessor (PHP), a general-purpose programming language suited for web development that can easily run on an online server, in order to subsequently analyze the data acquired during Phase 2 of the protocol.

2.5.1. Pre-Processing

Thanks to the motion artifacts generated by the jumps planned during the protocol, the portions of HBCG and ECG signals corresponding to each level of the imposed breathing protocol were identified.

2.5.2. Reference respiratory period duration from the ECG

After having identified the QRS complexes on the ECG signal using the Pan Tompkins method [30], the reference average $tRESP_{ECG}$ was obtained from the ECG signal by exploiting the amplitude modulation of the QRS complex peaks, following a pipeline inspired by Charlton et al [31]. Specifically, the ECG signal was low-pass filtered (cut-off frequency 1 Hz) to enhance the QRS complexes, facilitating the identification of local maxima and minima of QRS peaks' amplitude. Afterwards, the median distance between local maxima ($\widetilde{d}_{max}$) and the median distance between local minima ($\widetilde{d}_{min}$) were computed, and the $tRESP_{ECG}$ was computed according to the following formula:

$$tRESP_{ECG} = \left(\widetilde{\mathrm{d}}_{\max} + \widetilde{\mathrm{d}}_{\min}\right)/2 \tag{1}$$

2.5.3. Estimation of the respiratory period duration from the HBCG

The 6 channels of the HBCG signal, representing the time-varying position (PosX, PosY, PosZ) and the angular orientation (PosAngX, PosAngY, PosAngZ) along each axis of the subject's head, with respect to their initial position and orientation, were first down-sampled to 9 Hz to remove the high-frequency components (Fig. 3).

As previously introduced, in order to estimate in quasi-real-time the duration of each breathing period from such signals, an approach based on a grey-box parameter identification was developed, based on the parameters vector $\overrightarrow{p} = [p1, p2, p3, p4]$, where p1 is representative of the signal combination in input, p2 and p3 of the order of the Moving Average filter applied to smooth the noisy input signal, and for the consecutive applications of such filter, respectively, and p4 of the temporal window in which to search for peaks to prevent detecting possible artifacts.

The optimal values of the parameters in $\overrightarrow{p}$ were identified as those that minimize the Mean Relative Error (MRE) between the reference breathing period $tRESP_{ECG}$, and the algorithm's output estimate $tRESP_{HBCG}$ (Fig. 4).

As regards the parameter $p1$, 28 different combinations of signals were tested, as reported in Table 1.

The parameters $p2$ and $p3$ were relevant to a moving average (MA) filter applied to the combinations of input signals, as defined in Table 1. Specifically, $p2$ represents the consecutive samples used by the filter (i.e., its order), while $p3$ refers to the number of times the filter was consecutively applied. The possible values of $p2$, expressed in seconds, ranged from 0.5 s to 3.5 s with a step of 0.5 s (corresponding to a tested filter order of 4, 9, 13, 18, 22, 27, and 31 samples), while values of $p3$ were varied from 1 to 6. An example of a combination of signals ($p1 = 3$) obtained from one subject before and after the application of the MA filter, with $p2 = 1$ sec (MA filter order equal to 9) and $p3 = 2$ repetitions, is shown in Fig. 5 (top panel).

After application of the MA filter, local maxima and local minima were identified, and their time position saved. Subsequently, only the most prominent maxima in a range defined by the time interval

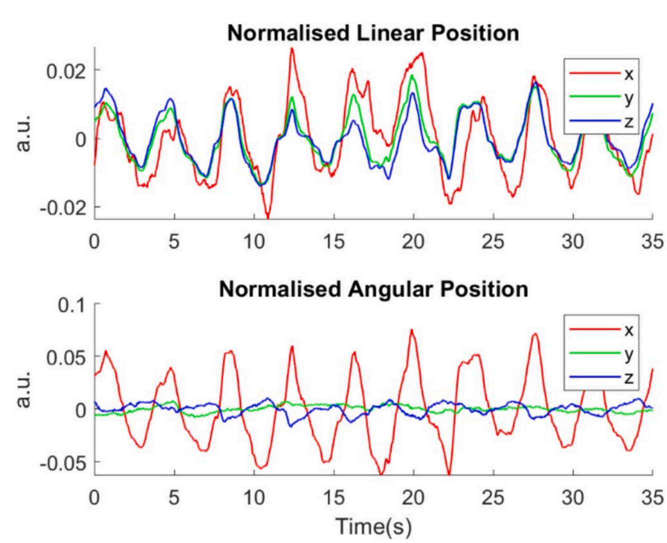

Fig. 3. Example of the signals representing the linear and angular positions of the VR headset, with respect to their initial position and orientation, after subsampling and normalization, used as input for further signal processing. It is possible to note the oscillations due to the breathing activity.

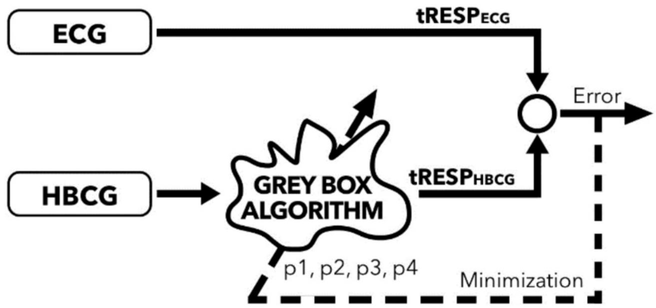

Fig. 4. Schematic of the proposed iterative minimization algorithm for the estimate of the best parameters vector (see text or details).

Table 1
List of the 28 combinations of linear (Pos) and angular (PosAng) positions considered as input for identification of the optimal value of $p1$.

	Signals Combination
1	$\left\|\overrightarrow{PosX}\right\|$
2	$\left\|\overrightarrow{PosY}\right\|$
3	$\left\|\overrightarrow{PosZ}\right\|$
4	$\left\|\overrightarrow{PosX}+\overrightarrow{PosY}\right\|$
5	$\left\|\overrightarrow{PosX}+\overrightarrow{PosZ}\right\|$
6	$\left\|\overrightarrow{PosY}+\overrightarrow{PosZ}\right\|$
7	$\left\|\overrightarrow{PosX}+\overrightarrow{PosY}+\overrightarrow{PosZ}\right\|$
8	$\left\|d\overrightarrow{PosX}/dt\right\|$
9	$\left\|d\overrightarrow{PosY}/dt\right\|$
10	$\left\|d\overrightarrow{PosZ}/dt\right\|$
11	$\left\|d(\overrightarrow{PosX}+\overrightarrow{PosY})/dt\right\|$
12	$\left\|d(\overrightarrow{PosX}+\overrightarrow{PosZ})/dt\right\|$
13	$\left\|d(\overrightarrow{PosY}+\overrightarrow{PosZ})/dt\right\|$
14	$\left\|d(\overrightarrow{PosX}+\overrightarrow{PosY}+\overrightarrow{PosZ})/dt\right\|$
15	$PosAngX$
16	$PosAngY$
17	$PosAngZ$
18	$PosAngX+PosAngY$
19	$PosAngX+PosAngZ$
20	$PosAngY+PosAngZ$
21	$PosAngX+PosAngY+PosAngZ$
22	$diff(PosAngX)$
23	$diff(PosAngY)$
24	$diff(PosAngZ)$
25	$diff(PosAngX+PosAngY)$
26	$diff(PosAngX+PosAngz)$
27	$diff(PosAngY+PosAngZ)$
28	$diff(PosAngx+PosAngY+PosAngZ)$

$[t_{max}-p4; t_{max}+p4]$, as well as the most prominent minima in the range $[t_{min}-p4; t_{min}+p4]$, were considered, with the parameter $p4$ ranging from 2 up to 3.5 s. An example of such detection with $p4=3$ s is shown in Fig. 5, bottom panel.

Lastly, the duration of the estimated respiratory cycle obtained by the HBCG signal ($tRESP_{HBCG}$) was estimated as follows:

$$tRESP_{HBCG}=\frac{median(diff(maxima))-median(diff(minima))}{2} \tag{2}$$

For each subject and for each level of the imposed respiration protocol, the parameters of vector $\overrightarrow{p}$ were evaluated across all possible combinations, in order to estimate the breathing period $\text{tRESP}_{\text{HBCG}}$. This result was subsequently compared with the reference value $\text{tRESP}_{\text{ECG}}$

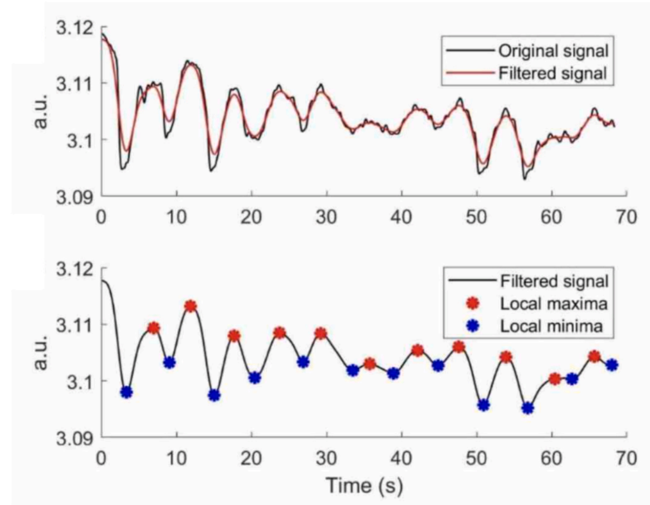

Fig. 5. Top: Combination of signals representing $\left|\overrightarrow{PosZ}\right|$, i.e. the absolute value of the Z head position (corresponding to$p1=3$), visualized before (in black) and after (in red) the MA filtering (with$p2=1$ s, i.e. MA filter order 9 and$p3=2$ repetitions). Bottom: Local maxima and local minima identified on the filtered combination of signals using$p4=3$ s. (For interpretation of the references to colour in this figure legend, the reader is referred to the web version of this article.)

obtained from the ECG. This extensive grid search algorithm aimed at identifying those parameters of $\overrightarrow{p}$ that minimize the MRE. Additionally, the bias and the standard deviation of the error were calculated for all the combinations of tested parameters.

2.6. Phase 2: Experimental protocol

Phase 2 of the protocol consisted in a VR experience during which the subject was initially prompted to choose both the duration (in minutes, between 1 and 5) of the breathing exercise and the imposed breathing cycle duration among the possible choices as described previously for Phase 1 (4 s, 6 s, 8 s, and 10 s per respiratory cycle). This was achieved by modifying the initial user interaction of the software developed for Phase 1, while all the remaining features, like the visual and the audio guide, remained unchanged.

At the end of the selected experience, the inertial signals acquired by the web app were forwarded to the server for the estimation of $\text{tRESP}_{\text{HBCG}}$, by utilizing the previously described grey-box algorithm with the corresponding optimal parameters obtained from Phase 1. A score was returned as a feedback to the subject, computed as:

$$Score=100-abs\left(\frac{tRESP_{HBCG}-tRESP_{imposed}}{tRESP_{imposed}}\right)\times 100 \tag{3}$$

As additional evaluation of the algorithm's performance, the Ecg-Move 4 device was also utilized during Phase 2: this allowed a post-hoc check of the estimated breathing period duration through a comparison with the one derived from the ECG signal.

2.7. Robustness analysis

In order to test the robustness of the grey-box algorithm in estimating $\text{tRESP}_{\text{HBCG}}$ in presence of noise, the following strategy was defined and applied to the data acquired from each of the 8 volunteers enrolled for Phase 2:

1) For each axial component i of the acquired position (PosX, PosY, PosZ) and angular orientation (PosAngX, PosAngY, PosAngZ), its standard deviation ($STDi$) was computed as reference;

2) Independent realizations of while noise were generated and multiplied by the corresponding *STDi* with a weight coefficient in the range 0.5 ÷ 4 and a step of 0.5;
3) The resulting signal was given as input to the grey-box algorithm set with the corresponding optimal parameters obtained from Phase 1;
4) The estimated $tRESP_{HBCG}$ was compared to the nominal imposed respiratory cycle duration.

In Fig. 6, a representative example of the acquired linear position signal from the VR headset without (top) and with white noise added, with increasing values of coefficient w (mid: w = 2; bottom: w = 4), where it is possible to observe the progressive degradation of the original information content.

3. Results

3.1. Phase 1: Parameters optimization

Two of the 26 participants enrolled during Phase 1 could not complete all the steps in the protocol because of hardware issues, and therefore 3 records (1 for one subject, 2 for the other subject) were discarded.

All the remaining records were successfully acquired resulting in a 97 % feasibility, and then used for the following analyses. An overview of the acquired data is summarized in Table 2.

After visual inspection of each acquired ECG and HBCG recorded signal, among the 101 recordings, 13 needed to be excluded because of a low-quality modulation and noise in the reference ECG signal, resulting in a total 87 % feasibility for the reference standard respiratory cycle duration obtained from the ECG.

The optimal values of the parameters of vector $\overrightarrow{p}^{*} = [p1, p2, p3, p4]$, resulting from the grey-box identification algorithm, for each level of the imposed breathing protocol, are summarized in Table 3. It is possible to notice that, for each level of the imposed breathing protocol, a different combination of parameters emerged as the preferred choice. Nevertheless, observing the computed indicators, these combinations resulted in similar and high performances, as shown in Table 4.

Table 2
Overview of the acquired records using the VR headset for each level of the imposed breathing protocol during phase 1 of the experiment, in which 12 respiratory cycles with the specified duration were elicited.

Protocol level	**L1**	**L2**	**L3**	**L4**	**Total**
Duration of the imposed respiratory cycle	4 *s*	6 *s*	8 *s*	10 *s*	
Number of records	26	26	25	24	101
Protocol duration	48 s	1 m 12 s	1 m 36 s	1 m 48 s	5 m 36 s
Total signal duration acquired (i.e., elapsed time)	39 m 34 s	44 m 14 s	56 m 31 s	63 m 55 s	3 h 24 *m*

Table 3
Optimal values of the parameters $p1$ (signals combination), $p2$ (MA filter order), $p3$ (number of repetitions of the MA filtering), $p4$ (minimum temporal distance between consecutive peaks) resulting from the gray-box identification algorithm as the best combination to estimate the respiratory cycle duration from the HBCG signals, compared to the reference value obtained from the ECG, for each protocol level (L1 = respiratory cycle duration 4 s; L2 = 6 s; L3 = 8 s, L4 = 10 s).

Protocol Level	$p1^{*}$	$p2^{*}$	$p3^{*}$	$p4^{*}$
L1	$\left\lvert\overrightarrow{PosX}+\overrightarrow{PosZ}\right\rvert$	4	4	2.5 s
L2	$\left\lvert\overrightarrow{PosX}+\overrightarrow{PosY}\right\rvert$	12	3	3 s
L3	$\left\lvert d\overrightarrow{PosZ}/dt\right\rvert$	27	4	3 s
L4	$\left\lvert d(\overrightarrow{PosY}+\overrightarrow{PosZ})/dt\right\rvert$	31	4	4 s

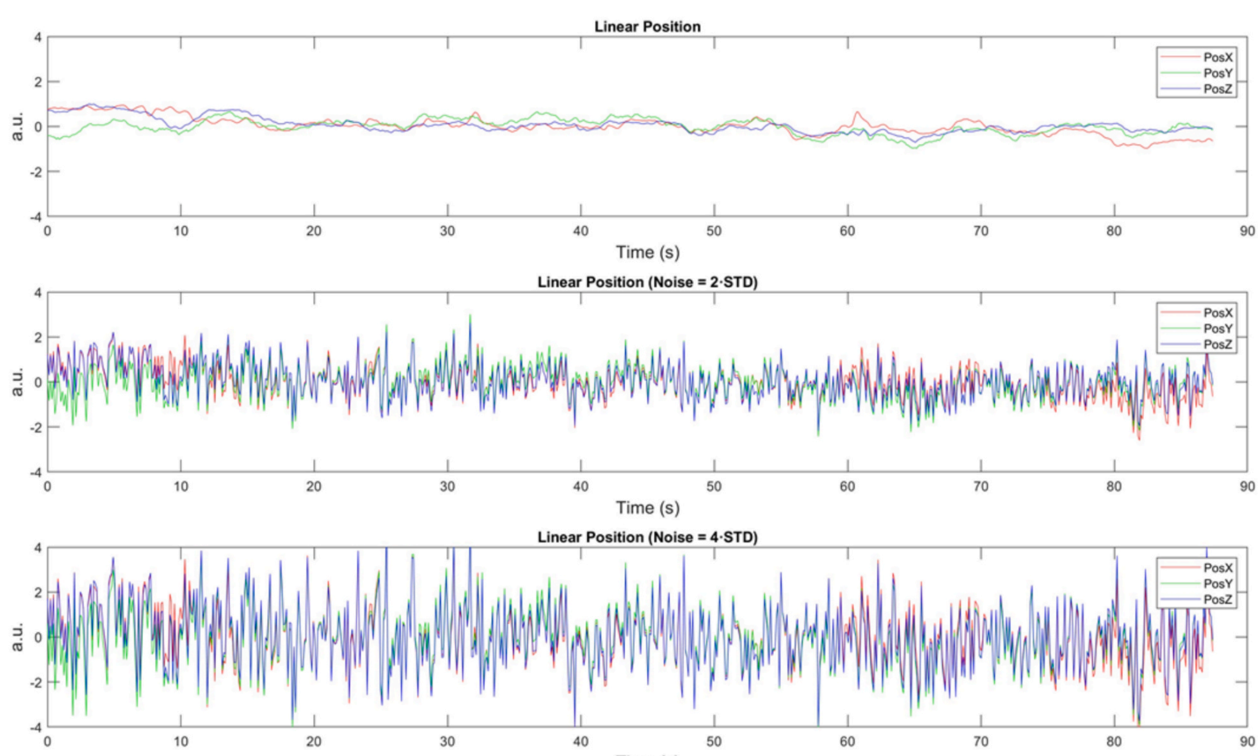

Fig. 6. Top: Representative example of the original linear position signal from Subject #2. Middle: the original signal with the added white noise with a weight = 2 applied. Bottom: the original signal with the added white noise with a weight = 4 applied.

Table 4
Performance of the estimation of the respiratory cycle duration from the HBCG signal, in comparison with the reference duration obtained by the ECG, using the combination of optimal parameters identified by the grey-box algorithm for each level of the protocol.

Protocol Level	Respiratory Cycle Duration	Mean Relative Error	Median Relative Error	Bias	Standard Deviation
L1	4 s	2.25 %	1.93 %	−0.02 s	0.14 s
L2	6 s	2.55 %	1.98 %	−0.06 s	0.21 s
L3	8 s	1.93 %	1.68 %	−0.11 s	0.19 s
L4	10 s	1.87 %	1.54 %	−0.11 s	0.26 s

3.2. Physiological confounders

To evaluate the potential influence of factors such as Body Mass Index (BMI), gender, and age on the HBCG signal and the respiratory rate estimation extracted by the VR headset, the correlation of such data with the mean relative error of the breathing period was computed for each protocol level using a linear model and computing the relevant coefficient of determination (r^2). Such analysis revealed no significant correlations, with values of $r^2 < 0.1$, thus indicating that the performance of the proposed algorithm for estimating the respiratory frequency from the VR headset is not subject to the examined physiological confounders.

3.3. Phase 2: Results of the algorithm testing

All the 8 healthy volunteers enrolled in Phase 2 of the protocol were able to satisfactorily complete it. The acquired HBCG signals were analyzed by using the previously tuned grey-box algorithm with the optimal combinations of the parameters relevant to the corresponding selected breathing cycle duration, thus resulting in the estimated $tRESP_{HBCG}$. The previously computed bias in the estimate as reported in Table 4 was used to correct it as follows:

$$tRESP^{*}_{HBCG} = tRESP_{HBCG} - bias \quad (4)$$

Table 5 shows, for each subject, the selected values for the duration of the VR experience and for the imposed breathing frequency. Also, $tRESP_{ECG}$ and the estimated $tRESP^{*}_{HBCG}$ are reported, together with the respective estimation error computed in comparison to the nominal imposed duration. It is worth noting that the frequency estimated from the HBCG was comparable (Wilcoxon Signed Rank test, p value = 1) to the one obtained from the reference ECG, and the individual estimate absolute error compared to the imposed nominal respiratory cycle duration was minimal and below 4 % in all the considered subjects.

3.4. Results of the robustness analysis

Table 6 reports the results relevant to the absolute error computed between the estimated $tRESP^*_{HBCG}$ (i.e., applying the respective bias correction as described in section 3.4) and the nominal imposed respiratory cycle, in % of the correct value, for the different levels of added noise in the eight examined subjects in Phase 2.

It is possible to observe an increasing trend (hence not for all subjects) in the measured error relevant to an increase in the noise amplitude, in particular when a weight >=2.5 was applied; in general, the error appeared acceptable in all subjects, with higher error values reported in subject #3.

In Fig. 7, an example of the output of the grey-box model, after application of the MA filter to the original linear position signal (in blue), as well as to the corrupted versions with increasing noise with w = 2 (in red) and w = 4 (in orange), is shown. It is possible to observe that, despite the added noise, the resulting morphology of the signals, and in particular the position of their peaks and valleys, were well overlapped, thus explaining the reduced absolute error between the estimated $tRESP^*_{HBCG}$ and the nominal imposed respiratory cycle, as shown in Table 6.

4. Discussion and Conclusions

In this work, an innovative and device-independent approach based on a web-based VR experience was presented, allowing the recording of the HBCG signal using the MEMS embedded in the VR headset while the user is exposed to a VE delivering an imposed respiration exercise. Specifically, the user's response to the protocol was estimated in terms of the mean duration of the respiratory cycle, providing direct feedback on the subject's performance immediately after the end of the session.

Even though VR headsets are not explicitly designed to acquire physiological signals, the utilization of the embedded inertial sensors enabled the measurement of the subject's head micromovements in 3D space, which are affected by respiratory activity. Indeed, thanks to an innovative parametric grey-box algorithm tuned by the data acquired during the training phase (Phase 1) and then translated into a general-purpose programming language suited to run on an external server used for the processing of the raw data coming from the VR headset, the proposed framework allowed a quasi-real-time estimation of subject's mean breathing period during the VR session, with a very high accuracy for the tested respiratory frequencies.

The results of this proof-of-concept study represent a first step towards the implementation of the VEE-Loop, as conceptualized in [20,21], for possible use in ecological momentary assessment of emotion elicitation through a VE, without the need to use external sensors.

In [22], the authors introduced the design of a general-purpose architecture for affective-driven procedural content generation in VR applications in mental health and wellbeing, validating it on 8 subjects. In their "The Emotional Labyrinth" VE, specific emotion-related features in a 3D maze were dynamically adapted according to a set of emotional states, demonstrating the feasibility of this approach. However, the VR experience was developed for HTC Vive (HTC, New Taipei City, Taiwan)

Table 5
Results of the processing of HBCG signals obtained during Phase 2 obtained with the optimized algorithm originated from Phase 1. The performance score presents the compliance of the subject with the imposed breathing protocol.

Subject	Duration (s)	Nominal respiratory cycle imposed (s/breath)	$tRESP_{ECG}$(s/breath)	$tRESP^{*}_{HBCG}$(s/breath)	Algorithm Error Vs Nominal (%)	Score
1	96	8	7.65	7.73	−3.37	96.6
2	96	8	8.09	7.94	−0.75	99.3
3	72	6	5.99	5.81	−3.17	96.8
4	96	10	9.52	9.79	−2.1	97.9
5	120	8	7.84	7.89	−1.37	98.6
6	96	8	8.09	7.94	−0.75	99.3
7	96	8	7.82	8.31	3.87	96.1
8	360	10	10.19	10.02	0.20	99.8

Table 6
Absolute error, both for each subject and cumulative, expressed as median and interquartile range (IQR), computed between the estimated tRESP*$_{HBCG}$ and the nominal imposed respiratory cycle, in % of the correct value. Noise amplitude with different standard deviation, modulated by the parameter weight (w), was added, and given as input to the optimized algorithm originated from Phase 1.

Subject/w	0.5	1	1.5	2	2.5	3	3.5	4
1	3 8 %	2.0 %	6.2 %	9.0 %	11.1 %	10.4 %	7.6 %	9.4 %
2	2.9 %	3.9 %	0.6 %	3.1 %	6.9 %	6.6 %	9.7 %	10.8 %
3	6.9 %	0.9 %	3.8 %	22.5 %	14.1 %	6.6 %	4.3 %	4.7 %
4	2.6 %	6.5 %	6.8 %	4.3 %	5.9 %	11.5 %	16.0 %	14.3 %
5	0.6 %	0.6 %	0.3 %	0.1 %	1.8 %	2.9 %	0.8 %	4.3 %
6	0.4 %	1.1 %	1.5 %	1.8 %	1.8 %	2.9 %	3.2 %	3.9 %
7	6.4 %	3.6 %	0.8 %	1.1 %	1.5 %	1.8 %	2.2 %	1.8 %
8	3.0 %	4.7 %	4.1 %	1.5 %	9.6 %	12.4 %	15.5 %	14.1 %
Median (IQR)	**2.9 (1.8)%**	**2.8 (3)%**	**2.6 (3.2)%**	**2.4 (2)%**	**6.4 (5.8)%**	**6.6 (4.9)%**	**5.9 (7.8)%**	**7.0 (7.4)%**

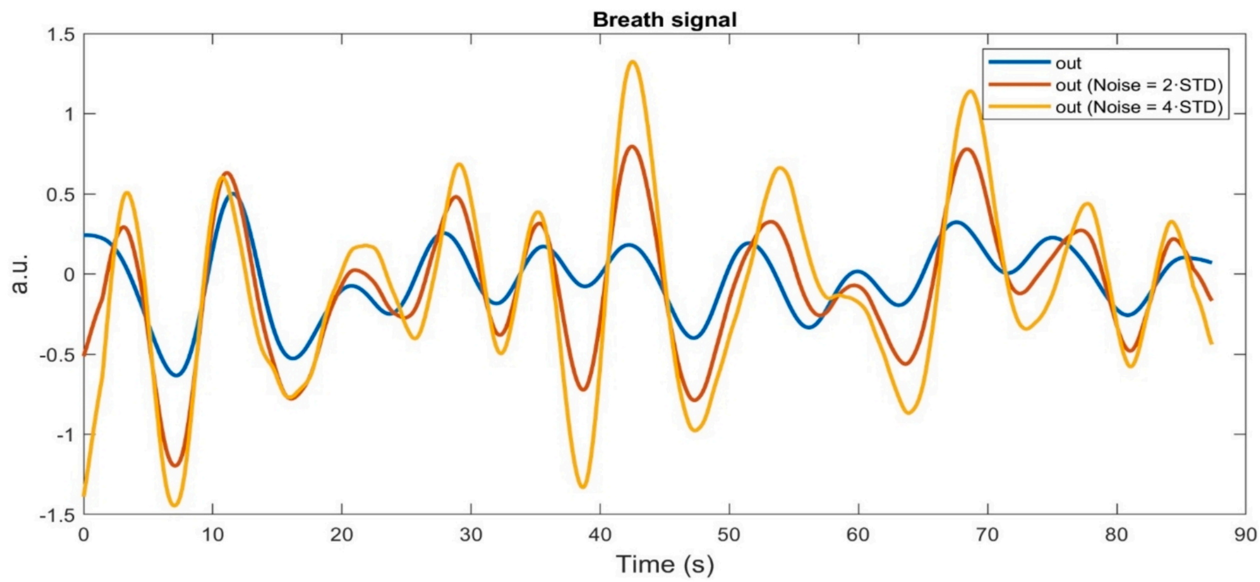

Fig. 7. Comparison of the signals generated as output from the grey-box algorithm when the signals presented in Fig. 6 were provided as input. It is possible to observe a good correspondence of peak and valleys in all three representations, from which the duration of the respiratory cycle was computed.

and a custom-made CAVE, with support to be executed as a traditional desktop application, and the proposed architecture requires the utilization of multiple wearable biosensors to determine the needed physiological markers, thus limiting the application to laboratory configurations.

In comparison, our approach introduces innovation as it proposes raw data acquisition in JavaScript from a web page, thus resulting device-independent by design. Additionally, thanks to the fact that it does not require any custom executable installation on the physical device nor a physical sensor to be put on the subject, it could be accessed from anywhere and utilized by the subject independently without the need for additional assistance, making it suitable for ecological momentary assessment.

The choice of the parametric grey-box algorithm was driven by the need to predefine the optimal values for the considered vector of parameters $\overrightarrow{p} = [p1, p2, p3, p4]$ to be then embedded in a lightweight version of the algorithm to be run on the external cloud and able to produce the relevant output in quasi-real time at the conclusion of the VR experience. A possible limitation of such an approach is represented by the strict dependence of the final results to the data used for training; however, the minimal absolute error found and the positive application to new data as in Phase 2 show the potential robustness of such approach when applied in normal subjects.

Also, the analysis conducted to test the robustness of the proposed method in resulting in an accurate estimation of the mean duration of the respiratory cycle showed good results, with an acceptable error in particular when the added noise amplitude was less than 2 times the SD of the original signals. This behavior could be attributed to the proper values of the coefficients *p2* (MA filter order) and *p3* (number of repetitions of the MA filtering) in the gray-box algorithm, which allowed the effective filtering of the noise even in presence of unfavorable conditions.

At this stage, a full real-time implementation (i.e., giving as output a continuous update of the current respiratory frequency during the VR experience) was not feasible with the tested VR headset because of the lags caused by the high computational demand of such kind of algorithm, which would have inevitably increased the risk of motion sickness in the subjects wearing the headset.

Interestingly, even though the signals recorded with both the accelerometer and the gyroscope were considered, the best results were achieved using combinations of the signals acquired with the accelerometer for all the four tested imposed breathing frequencies. As the VR experience was constituted by a sphere still in its centered position in the 3D space, with changes in its size (without any rotation) synchronous with the sinusoidal frequency corresponding to the imposed breathing frequency, we could hypothesize that rotational head movements were minimized, with subject's attention focused on the visual guide during the protocol. As such, the observed main component of respiratory activity on the head in sitting position could be related to the inspiratory/expiratory pattern that resulted in a motion with a more accentuated translational component (head-to-foot and front-to-back). This aspect will need to be further investigated in future studies involving subjects in free breathing while immersed in a VE.

Our study has several limitations: 1) it was conducted with participants in a seated position and following an imposed breathing pattern, so that the performance of the algorithm in more realistic scenarios, with natural breathing patterns and different postures, remains to be evaluated. 2) The evaluation of a larger sample size would have increased statistical power and generalizability of our findings. However, this study serves as proof-of-concept for what proposed, leaving to future studies its application in similar protocols applied to large subjects groups. (3) While ECG-derived respiratory rate, as the reference standard for validating the HBCG-derived respiratory rate, is a widely accepted method for such estimate, it is not the gold standard: direct measurement of respiratory airflow or chest wall movements could have provided a more precise reference for comparison. However, our choice was driven to limit synchronization problems among independent devices. 4) The study does not explicitly address the potential impact of motion artifacts or head movements unrelated to respiration on the HBCG signal and the subsequent respiratory rate estimation. This could be a potential source of error, especially in more dynamic or unconstrained settings. 5) An imposed breathing protocol was used in the controlled laboratory setting of the study. Establishing the practical utility and robustness of the proposed approach would require further validation in real-world scenarios, with diverse user populations and various virtual reality experiences. 6) The method lacks validation in specific populations (e.g., individuals requiring respiratory training), as it has been applied to normal volunteers only. Modification of the respiratory protocol embedded in the VR scenario and its application for testing to specific patients' populations will be the focus of future research.

Despite being limited to monitoring the respiratory activity performance during imposed breathing, our results represent a proof-of-concept towards the development of VEs with possible clinical applications, to be utilized remotely by the patient in those situations in which respiratory activity monitoring is deemed important.

The respiratory frequency is indeed considered a fundamental variable to be monitored in different situations [32], providing information on clinical deterioration [33], predicting cardiac arrest [34,35], and supporting the diagnosis of severe pneumonia [36,37]. Moreover, respiratory rate responds to a variety of stressors, including emotional stress [38,39,40], and cognitive load [41], and represents an effective marker of physical effort and fatigue during exercise [42,43,44]. Despite the technological development in the field of sensors and the growing number of techniques and measurement solutions for measuring respiratory rate [45], one of the main commonly highlighted challenges is represented by the limited use of respiratory systems in everyday-life monitoring.

The upcoming widespread diffusion of VR headsets, together with the design of application-specific VE aimed at monitoring respiratory frequency by the proposed method, could represent an additional ubiquitous tool to engage the patients in such activity. Such approach could be used for testing procedures for out-of-lab diagnosis [46], to assess clinical deterioration for a variety of pathological conditions [47], as well as to identify emotional states in a variety of conditions and populations [48]. As well, the assessment of respiratory frequency during static working activities simulated through serious gaming VE could be used to quantify the cognitive load, and potential beneficial effect of training [49].

The choice of implementing a VE scenario based on voluntary modulation of breathing, guided by the synchronized sound and real-time display of a 3D shape, was driven by the fact that such maneuvers have been shown to lead to a series of systemic effects inducing potential benefits in a range of disorders, such as decreasing blood pressure in patients with hypertension [50], reducing stress, anxiety and pain [51], improving health-related quality of life in heart failure patients [52], and favoring therapy delivery while minimizing side effects in tumor patients undergoing radiotherapy [53]. The promising results obtained in our protocol, with respiratory frequencies capable of producing marked systemic effects [54], show the potential application of similar VE protocols to further study in specific patient populations the expected beneficial effects.

In conclusion, this proof-of-concept study presented an innovative device-independent web-based VR experience in which the HBCG signal was acquired through the embedded MEMS during an imposed breathing protocol by audio-visual guidance. The mean respiratory period duration was estimated by a tuned grey-box algorithm and used to measure the user's performance in the proposed tasks, presented as biofeedback in quasi-real time at the end of the session, without the need for any external sensor. With the proposed approach, the individual estimate absolute error compared to the imposed nominal respiratory cycle duration was minimal and below 4 % in all the considered subjects. These results represent a proof-of-concept towards the development of VEs for possible use in ecological momentary assessment with possible clinical applications, to be utilized remotely by the patient in those situations in which respiratory activity monitoring is deemed important.

CRediT authorship contribution statement

Andrea Carpi: Writing – original draft, Visualization, Software, Investigation, Data curation. **Sarah Solbiati:** Writing – review & editing, Validation, Investigation, Formal analysis. **Valentino Megale:** Writing – review & editing, Conceptualization. **Enrico Gianluca Caiani:** Conceptualization, Methodology, Resources, Supervision, Writing – original draft, Writing – review & editing.

Declaration of competing interest

The authors declare that they have no known competing financial interests or personal relationships that could have appeared to influence the work reported in this paper.

Data availability

Data could be made available on reasonable request.

References

[1] A.Y. Nee, S.K. Ong, Virtual and augmented reality applications in manufacturing, IFAC Proceedings Volumes. 46 (9) (2013 Jan 1) 15–26, https://doi.org/10.3182/20130619-3-RU-3018.00637.
[2] M. Slater, M.V. Sanchez-Vives, Enhancing our lives with immersive virtual reality, Front. Rob. AI 19 (3) (2016 Dec) 74, https://doi.org/10.3389/frobt.2016.00074.
[3] J. Aida, B. Chau, J. Dunn, Immersive virtual reality in traumatic brain injury rehabilitation: a literature review, NeuroRehabilitation 42 (4) (2018 Jan 1) 441–448, https://doi.org/10.3233/NRE-172361.
[4] J.L. Maples-Keller, C. Yasinski, N. Manjin, B.O. Rothbaum, Virtual reality-enhanced extinction of phobias and post-traumatic stress, Neurotherapeutics 14 (2017 Jul) 554–563, https://doi.org/10.1007/s13311-017-0534-y.
[5] B. Spiegel, G. Fuller, M. Lopez, T. Dupuy, B. Noah, A. Howard, M. Albert, V. Tashjian, R. Lam, J. Ahn, F. Dailey, Virtual reality for management of pain in hospitalized patients: A randomized comparative effectiveness trial, PLoS One 14 (8) (2019 Aug 14) e0219115, https://doi.org/10.1371/journal.pone.0219115.
[6] S.M. Schneider, C.K. Kisby, E.P. Flint, Effect of virtual reality on time perception in patients receiving chemotherapy, Support. Care Cancer 19 (2011 Apr) 555–564, https://doi.org/10.1007/s00520-010-0852-7.
[7] L.D. Morris, Q.A. Louw, K. Grimmer-Somers, The effectiveness of virtual reality on reducing pain and anxiety in burn injury patients: a systematic review, Clin. J. Pain 25 (9) (2009 Nov 1) 815–826, https://doi.org/10.1097/AJP.0b013e3181aaa909.
[8] Gold JI, Kant AJ, Kim SH. Virtual anesthesia: the use of virtual reality for pain distraction during acute medical interventions. InSeminars in Anesthesia, Perioperative Medicine and Pain 2005 Dec 1 (Vol. 24, No. 4, pp. 203-210). WB Saunders. doi: 10.1053/j.sane.2005.10.005.
[9] E. Furman, T.R. Jasinevicius, N.F. Bissada, K.Z. Victoroff, R. Skillicorn, M. Buchner, Virtual reality distraction for pain control during periodontal scaling and root planing procedures, J. Am. Dent. Assoc. 140 (12) (2009 Dec 1) 1508–1516, https://doi.org/10.14219/jada.archive.2009.0102.
[10] S. Farra, E. Hodgson, E.T. Miller, N. Timm, W. Brady, M. Gneuhs, J. Ying, J. Hausfeld, E. Cosgrove, A. Simon, M. Bottomley, Effects of virtual reality simulation on worker emergency evacuation of neonates, Disaster Med. Public Health Prep. 13 (2) (2019 Apr) 301–308, https://doi.org/10.1017/dmp.2018.58.

[11] V.C. Pandrangi, B. Gaston, N.P. Appelbaum, F.C. Albuquerque Jr, M.M. Levy, R. A. Larson, The application of virtual reality in patient education, Ann. Vasc. Surg. 1 (59) (2019 Aug) 184–189, https://doi.org/10.1016/j.avsg.2019.01.015.

[12] S. Rourke, How does virtual reality simulation compare to simulated practice in the acquisition of clinical psychomotor skills for pre-registration student nurses? A systematic review, Int. J. Nurs. Stud. 1 (102) (2020 Feb) 103466, https://doi.org/10.1016/j.ijnurstu.2019.103466.

[13] Brunnström K, Beker SA, De Moor K, Dooms A, Egger S, Garcia MN, Hossfeld T, Jumisko-Pyykkö S, Keimel C, Larabi MC, Lawlor B. Qualinet white paper on definitions of quality of experience. https://hal.science/hal-00977812/.

[14] M.V. Sanchez-Vives, M. Slater, From presence to consciousness through virtual reality, Nat. Rev. Neurosci. 6 (4) (2005 Apr 1) 332–339, https://doi.org/10.1038/nrn1651.

[15] M. Slater, Place illusion and plausibility can lead to realistic behaviour in immersive virtual environments, Philos. Trans. R. Soc., B 364 (1535) (2009 Dec 12) 3549–3557, https://doi.org/10.1098/rstb.2009.0138.

[16] M. Slater, S. Wilbur, A framework for immersive virtual environments (FIVE): Speculations on the role of presence in virtual environments, Presence Teleop. Virt. 6 (6) (1997 Dec 1) 603–616, https://doi.org/10.1162/pres.1997.6.6.603.

[17] Hupont I, Gracia J, Sanagustin L, Gracia MA. How do new visual immersive systems influence gaming QoE? A use case of serious gaming with Oculus Rift. In2015 Seventh international workshop on quality of multimedia experience (QoMEX) 2015 May 26 (pp. 1-6). IEEE. doi: 10.1109/QoMEX.2015.7148110.

[18] Li HC, Seo J, Kham K, Lee S. Measurement of 3D visual fatigue using event-related potential (ERP): 3D oddball paradigm. In2008 3DTV conference: the true vision-capture, transmission and display of 3D video 2008 May 28 (pp. 213-216). IEEE. doi: 10.1109/3DTV.2008.4547846.

[19] E. Kroupi, P. Hanhart, J.S. Lee, M. Rerabek, T. Ebrahimi, Modeling immersive media experiences by sensing impact on subjects, Multimed. Tools Appl. 75 (2016 Oct) 12409–12429, https://doi.org/10.1007/s11042-015-2980-zm.

[20] Andreoletti D, Luceri L, Peternier A, Leidi T, Giordano S. The virtual emotion loop: towards emotion-driven product design via virtual reality. In2021 16th Conference on Computer Science and Intelligence Systems (FedCSIS) 2021 Sep 2 (pp. 371-378). IEEE. doi: 10.15439/2021F120.

[21] Andreoletti D, Paoliello M, Luceri L, Leidi T, Peternier A, Giordano S. A framework for emotion-driven product design through virtual reality. InSpecial Sessions in the Advances in Information Systems and Technologies Track of the Conference on Computer Science and Intelligence Systems 2021 Sep 2 (pp. 42-61). Cham: Springer International Publishing. doi: 10.1007/978-3-030-98997-2_3.

[22] S.B. Badia, L.V. Quintero, M.S. Cameirao, A. Chirico, S. Triberti, P. Cipresso, A. Gaggioli, Toward emotionally adaptive virtual reality for mental health applications, IEEE J. Biomed. Health Inform. 23 (5) (2018 Oct 31) 1877–1887, https://doi.org/10.1109/JBHI.2018.2878846.

[23] Da He D, Winokur ES, Sodini CG. A continuous, wearable, and wireless heart monitor using head ballistocardiogram (BCG) and head electrocardiogram (ECG). In2011 Annual International Conference of the IEEE engineering in medicine and biology society 2011 Aug 30 (pp. 4729-4732). IEEE. doi: 10.1109/IEMBS.2011.6091171.

[24] Da He D, Winokur ES, Sodini CG. An ear-worn continuous ballistocardiogram (BCG) sensor for cardiovascular monitoring. In2012 Annual International Conference of the IEEE Engineering in Medicine and Biology Society 2012 Aug 28 (pp. 5030-5033). IEEE. doi: 10.1109/EMBC.2012.6347123.

[25] Hernandez J, Li Y, Rehg JM, Picard RW. Cardiac and respiratory parameter estimation using head-mounted motion-sensitive sensors. EAI Endorsed Transactions on Pervasive Health and Technology. 2015 May 18;1(1):e2-. doi: 10.4108/phat.1.1.e2.

[26] Hernandez J, McDuff DJ, Picard RW. BioInsights: Extracting personal data from "Still" wearable motion sensors. In2015 IEEE 12th International Conference on Wearable and Implantable Body Sensor Networks (BSN) 2015 Jun 9 (pp. 1-6). IEEE. doi: 10.1109/BSN.2015.7299354.

[27] C. Floris, S. Solbiati, F. Landreani, G. Damato, B. Lenzi, V. Megale, E.G. Caiani, Feasibility of heart rate and respiratory rate estimation by inertial sensors embedded in a virtual reality headset, Sensors 20 (24) (2020 Dec 14) 7168, https://doi.org/10.3390/s20247168.

[28] Solbiati S, Buffoli A, Megale V, Damato G, Lenzi B, Langfelder G, Caiani EG. Detecting Heart Rate From Virtual Reality Headset-Embedded Inertial Sensors: a Kinetic Energy Approach. In 2021 International Conference on e-Health and Bioengineering (EHB) 2021 Nov 18 (pp. 1-4). IEEE. doi: 10.1109/EHB52898.2021.9657564.

[29] Solbiati S, Buffoli A, Megale V, Damato G, Lenzi B, Langfelder G, Caiani EG. Monitoring Cardiac Activity by Detecting Subtle Head Movements Using MEMS Technology. In 2022 IEEE International Symposium on Inertial Sensors and Systems (INERTIAL) 2022 May 8 (pp. 1-4). IEEE. doi: 10.1109/INERTIAL53425.2022.9787725.

[30] J. Pan, W.J. Tompkins, A Real-Time QRS Detection Algorithm. IEEE Ttransactions on, Biomed. Eng. (1985).

[31] P.H. Charlton, D.A. Birrenkott, T. Bonnici, M.A.F. Pimentel, A.E.W. Johnson, J. Alastruey, L. Tarassenko, P.J. Watkinson, R. Beale, D.A. Clifton, Breathing Rate Estimation from the Electrocardiogram and Photoplethysmogram: A Review, IEEE Rev Biomed Eng. 11 (2018) 2–20.

[32] A. Nicolò, C. Massaroni, E. Schena, M. Sacchetti, The importance of respiratory rate monitoring: From healthcare to sport and exercise, Sensors 20 (21) (2020 Nov 9) 6396, https://doi.org/10.3390/s20216396.

[33] M.A. Cretikos, R. Bellomo, K. Hillman, J. Chen, S. Finfer, A. Flabouris, Respiratory rate: the neglected vital sign, Med. J. Aust. 188 (11) (2008 Jun) 657–659, https://doi.org/10.5694/j.1326-5377.2008.tb01825.x.

[34] M.M. Churpek, T.C. Yuen, S.Y. Park, D.O. Meltzer, J.B. Hall, D.P. Edelson, Derivation of a cardiac arrest prediction model using ward vital signs, Crit. Care Med. 40 (7) (2012 Jul) 2102, https://doi.org/10.1097/CCM.0b013e318250aa5a.

[35] J.F. Fieselmann, M.S. Hendryx, C.M. Helms, D.S. Wakefield, Respiratory rate predicts cardiopulmonary arrest for internal medicine inpatients, J. Gen. Intern. Med. 8 (1993 Jul) 354–360, https://doi.org/10.1007/BF02600071.

[36] D. Goodman, M.E. Crocker, F. Pervaiz, E.D. McCollum, K. Steenland, S. M. Simkovich, C.H. Miele, L.L. Hammitt, P. Herrera, H.J. Zar, H. Campbell, Challenges in the diagnosis of paediatric pneumonia in intervention field trials: recommendations from a pneumonia field trial working group, Lancet Respir. Med. 7 (12) (2019 Dec 1) 1068–1083, https://doi.org/10.1016/S2213-2600(19)30249-8.

[37] C. Massaroni, A. Nicolò, E. Schena, M. Sacchetti, Remote respiratory monitoring in the time of COVID-19, Front. Physiol. 29 (11) (2020 May) 635, https://doi.org/10.3389/fphys.2020.00635.

[38] S.A. Shea, Behavioural and arousal-related influences on breathing in humans, Experimental Physiology: Translation and Integration. 81 (1) (1996 Jan 1) 1–26, https://doi.org/10.1113/expphysiol.1996.sp003911.

[39] M.J. Tipton, A. Harper, J.F. Paton, J.T. Costello, The human ventilatory response to stress: rate or depth? J. Physiol. 595 (17) (2017 Sep 1) 5729–5752, https://doi.org/10.1113/JP274596.

[40] I. Homma, Y. Masaoka, Breathing rhythms and emotions, Exp. Physiol. 93 (9) (2008 Sep 1) 1011–1021, https://doi.org/10.1113/expphysiol.2008.042424.

[41] M. Grassmann, E. Vlemincx, A. Von Leupoldt, J.M. Mittelstädt, O. Van den Bergh, Respiratory changes in response to cognitive load: A systematic review, Neural Plast. 1 (2016 Jan) 2016, https://doi.org/10.1155/2016/8146809.

[42] A. Nicolò, M. Girardi, I. Bazzucchi, F. Felici, M. Sacchetti, Respiratory frequency and tidal volume during exercise: differential control and unbalanced interdependence, Physiol. Rep. 6 (21) (2018 Nov) e13908, https://doi.org/10.14814/phy2.13908.

[43] A. Nicolò, S.M. Marcora, M. Sacchetti, Respiratory frequency is strongly associated with perceived exertion during time trials of different duration, J. Sports Sci. 34 (13) (2016 Jul 2) 1199–1206, https://doi.org/10.1080/02640414.2015.1102315.

[44] A. Nicolò, C. Massaroni, L. Passfield, Respiratory frequency during exercise: the neglected physiological measure, Front. Physiol. 11 (8) (2017 Dec) 922, https://doi.org/10.3389/fphys.2017.00922.

[45] E. Vanegas, R. Igual, I. Plaza, Sensing systems for respiration monitoring: A technical systematic review, Sensors 20 (18) (2020 Sep 22) 5446, https://doi.org/10.3390/s20185446.

[46] K. Wasserman, R. Casaburi, Dyspnea: physiological and pathophysiological mechanisms, Annu. Rev. Med. 39 (1) (1988 Feb) 503–515, https://doi.org/10.1146/annurev.me.39.020188.002443.

[47] G.B. Smith, D.R. Prytherch, P. Meredith, P.E. Schmidt, P.I. Featherstone, The ability of the National Early Warning Score (NEWS) to discriminate patients at risk of early cardiac arrest, unanticipated intensive care unit admission, and death, Resuscitation 84 (4) (2013 Apr 1) 465–470, https://doi.org/10.1016/j.resuscitation.2012.12.016.

[48] Q. Zhang, X. Chen, Q. Zhan, T. Yang, S. Xia, Respiration-based emotion recognition with deep learning, Comput. Ind. 1 (92) (2017 Nov) 84–90, https://doi.org/10.1016/j.compind.2017.04.005.

[49] R.S. Bridger, K. Brasher, Cognitive task demands, self-control demands and the mental well-being of office workers, Ergonomics 54 (9) (2011 Sep 1) 830–839, https://doi.org/10.1080/00140139.2011.596948.

[50] M.H. Schein, B. Gavish, M. Herz, D. Rosner-Kahana, P. Naveh, B. Knishkowy, E. Zlotnikov, N. Ben-Zvi, R.N. Melmed, Treating hypertension with a device that slows and regularises breathing: a randomised, double-blind controlled study, J. Hum. Hypertens. 15 (4) (2001 Apr) 271–278, https://doi.org/10.1038/sj.jhh.1001148.

[51] R.P. Brown, P.L. Gerbarg, F. Muench, Breathing practices for treatment of psychiatric and stress-related medical conditions, Psychiatr. Clin. 36 (1) (2013 Mar 1) 121–140, https://doi.org/10.1016/j.psc.2013.01.001.

[52] G. Parati, G. Malfatto, S. Boarin, G. Branzi, G. Caldara, A. Giglio, G. Bilo, G. Ongaro, A. Alter, B. Gavish, G. Mancia, Device-guided paced breathing in the home setting: effects on exercise capacity, pulmonary and ventricular function in patients with chronic heart failure: a pilot study, Circ. Heart Fail. 1 (3) (2008 Sep 1) 178–183, https://doi.org/10.1161/CIRCHEARTFAILURE.108.772640.

[53] George R, Chung TD, Vedam SS, Ramakrishnan V, Mohan R, Weiss E, Keall PJ. Audio-visual biofeedback for respiratory-gated radiotherapy: impact of audio instruction and audio-visual biofeedback on respiratory-gated radiotherapy. International Journal of Radiation Oncology* Biology* Physics. 2006 Jul 1;65(3):924-33. doi: 10.1016/j.ijrobp.2006.02.035.

[54] J. Pagaduan, S.S. Wu, T. Kameneva, E. Lambert, Acute effects of resonance frequency breathing on cardiovascular regulation, Physiol. Rep. 7 (22) (2019 Nov) e14295, https://doi.org/10.14814/phy2.14295.